Tight-Binding based SiGe Band Structure Calculations and Implication on Transport

Saumitra Mehrotra, Abhijeet Paul, Gerhard Klimeck, and Mathieu Luisier
School of Electrical and Computer Engineering, Network for Computational Nanotechnology,
and Birck Nanotechnology Center, Purdue University, West Lafayette, IN, USA - 47907
Email: smehrotr@purdue.edu

***Abstract*— This work presents a comprehensive analysis of the SiGe band structure using a Tight-Binding based approach within the virtual crystal approximation. We analyze the material properties of bulk relaxed SiGe and biaxially compressed strained systems. The simulation approach has been benchmarked against experimental data wherever possible. We further investigate the effect of process induced uniaxial strain in <100> SiGe/Si pMOS devices. It is found that uniaxial strain can further improve the performance of biaxially compressed SiGe/Si based pMOS devices by as much as 10% for high Ge% devices.**

Keywords- SiGe, biaxial, uniaxial strain, bandstructure.

I. INTRODUCTION

The continuous shrinking of channel lengths (Lc) in silicon CMOS devices to increase their performance has led to the exploration of new high mobility channel materials. Ge exhibits higher hole mobility compared to Si. However, due to the difficulties in fabricating a suitable dielectric in Ge based devices, the focus has been redirected towards SiGe. About 30% hole mobility enhancement relative to unstrained Si [1] have been demonstrated in biaxially compressed SiGe/Si channel materials. Strained SiGe pMOS devices are being considered as one of the designs for the ultimate CMOS [2].

So far device engineers have mostly employed the k•p method to model transport in bulk transistors.. Here we present a Tight-Binding (TB) based bandstructure calculation method in the virtual crystal approximation (VCA) [3] for bulk relaxed and strained SiGe/Si material systems. Section II provides a brief description of the TB-VCA model used for calculation of electronic structure.

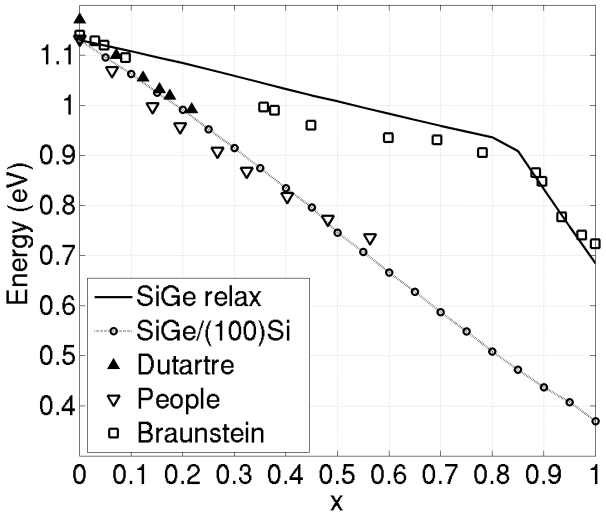

Figure 1. Bandgaps computed for relaxed $Si_{1-x}Ge_x$ and $Si_{1-x}Ge_x$/Si using TB-VCA model. Experimental data from [4][5][6].

Section III discusses the bandgaps/bandedges. In Section IV we talk about the variations in electron and hole effective masses. Finally in Section V we talk about uniaxial strain as a performance booster in SiGe/Si pMOS devices.

II. TIGHT-BINDING VCA MODEL

SiGe is a binary alloy composed of Si and Ge atomic species. In the virtual crystal approximation the alloy is represented as an 'averaged' atom which has the averaged properties of the individual atomic species.

The sp3d5s* tight-binding parameters for Si and Ge [7] are scaled as below for $Si_{1-x}Ge_x$ ($0<x<1$). Here E represents the onsite energy for the orbital σ while V represents the nearest neighbour σ1-σ2 orbital coupling energy.

$$E_{\sigma}^{SiGe} = (1-x).E_{\sigma}^{Si} + x.E_{\sigma}^{Ge} \quad (1)$$

$$V_{\sigma 1\sigma 2}^{SiGe} = (1-x).V_{\sigma 1\sigma 2}^{Si} + x.V_{\sigma 1\sigma 2}^{Ge} \quad (2)$$

For the strained case the individual parameters are scaled according to Harrison's scaling rule [8]. Lattice

constant (d^{SiGe}) of Si_xGe_{1-x} is linearly interpolated according to Vegard's law.

$$d^{SiGe} = x.d^{Si} + (1-x)d^{Ge} \quad (3)$$

III. BANDGAPS AND BANDEDGES

Bandstructure of bulk $Si_{1-x}Ge_x$ exhibits a Si like conduction band (CB) minima along X for x<0.85. The material has Ge like character with conduction band minima along L when x>0.85.This crossover from X to L valley is correctly captured in the TB-VCA model (Fig. 2).

SiGe when pseudomorphically grown on relaxed Si substrate is biaxially compressed due to about 4% lattice mismatch between Ge and Si. The compressive strain splits the six-fold degenerate CB X valleys into set of Δ_4 and Δ_2 valleys. The in-plane Δ_4 forms the lowest energy level and is the

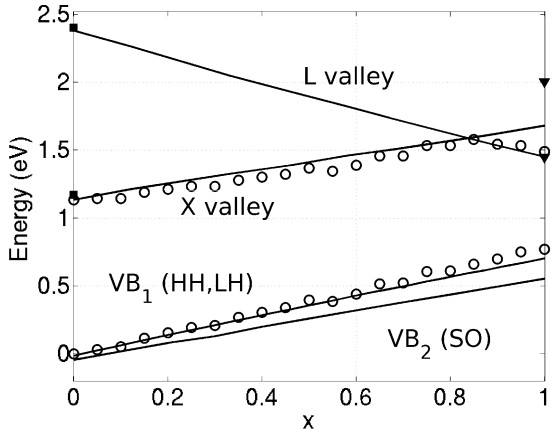

Figure 2. Calculated bandedges for relaxed bulk relaxed $Si_{1-x}Ge_x$ Experimental references (■) (▼) from [9]. CB and VB data from [10],[11].

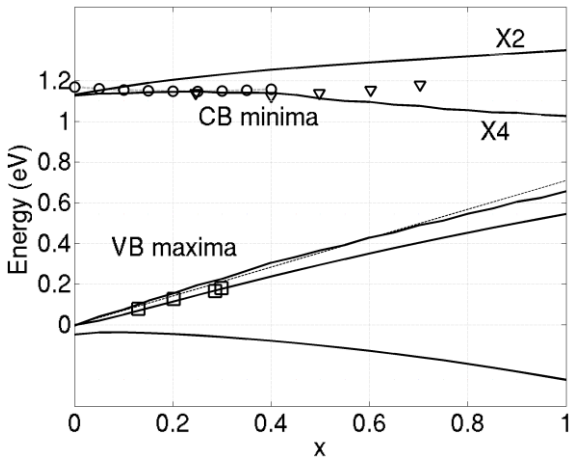

Figure 3. Calculated bandedges for $Si_{1-x}Ge_x$/(100)Si. Experimental references from (o) [13], (Δ) [6], (□) [12].

conduction band edge of $Si_{1-x}Ge_x$ for all x. The loss of symmetry due to the application of strain splits the degenerate heavy hole (hh) and light hole (lh) valence bands (VB) at the Γ point. The lowering of Δ_4 energy level leads to the formation of Type I heterostructure with a large valence band offset and small conduction band offset (Fig. 3). Valence band edge increases linearly in energy with increasing Ge% leading to a smaller bandgap with compressive strain. Fully strained Ge/Si has an estimated bandgap of about 0.37eV.

IV. EFFECTIVE MASS

The effective mass is an important parameter that strongly influences device properties. Fig. 4 shows the electron masses computed for the relaxed and strained cases. The longitudinal and transverse mass for lowest CB X and L valleys do not exhibit appreciable change.

Contrary to the electron masses, the hole masses show large variations with application of strain. Compressive strain causes lifting of degenerate hh and lh bands. The higher energy band shows a lower in-plane and relatively higher out-of-plane effective mass. This feature is important in pMOS devices transport because of small transport mass and larger density of states (DOS) / confinement mass. Fig. 5 shows highest valence band of bulk Si, $Si_{50}Ge_{50}$/Si, Ge/Si and $Si_{50}Ge_{50}$/Si with further application of 1% compressive uniaxial strain. Notice that heavy and light hole bands are degenerate for Si but we here show only the heavy hole.

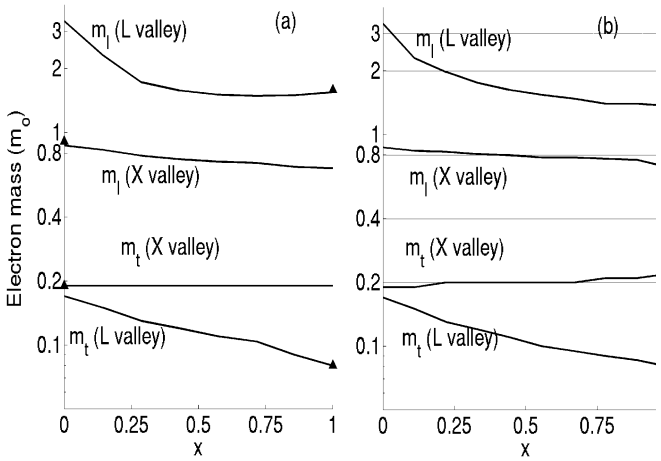

Figure 4. Calculated transverse (m_t) and longitudinal (m_l) electron masses for X and L valleys for (a) relax $Si_{1-x}Ge_x$ and (b) $Si_{1-x}Ge_x$/ (100) Si. Experimental data from [9].

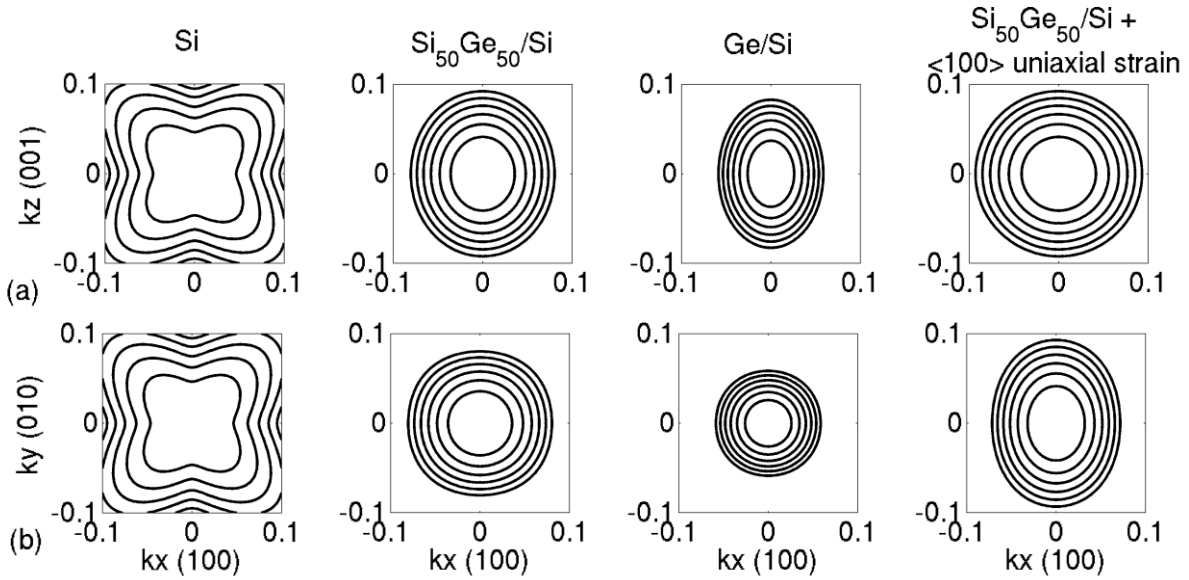

Figure 5. Out-of-plane (a) and in-plane (b) E-k diagram (energy contours from 1-5 meV) for bulk Si, $Si_{50}Ge_{50}$/(001)Si, Ge/Si and $Si_{50}Ge_{50}$/(001)Si with 1% <100> compressive uniaxial strain.

exhibits different and larger mass along <110> as compared to <100> direction. As soon as strain is applied the warping is lost near the valence band edge. In the case of biaxial strain, the valence band edge becomes isotropic and parabolic near Γ. From Fig 5. (a) it can be inferred that uniaxial strain affects the in-plane bandstructure more than the out-of-plane bandstructure. Uniaxial strain further reduces transport effective mass without affecting the DOS mass. Fig. 6 shows the computed effective DOS mass and transport mass along <100>. The fffective DOS mass is computed using (4) taking into account DOS due to second top most band.

$$m_{dos}^{eff} = m_{001}^{v1} + m_{001}^{v2}.\exp\left(\frac{-\Delta E_{v,split}}{k_b T}\right) \qquad (4)$$

$\Delta E_{v,split}$ is the difference in energy between the two top valence bands.

The effect of uniaxial strain can be seen in Fig. 7. The effective valence DOS mass shows a slight reduction due to the splitting of top two valence bands. However the isotropic in-plane mass changes for <010> and <100> directions <100> oriented mass being smaller than original value. The <100> transport mass reduces quickly for, even small amount of uniaxial strain. At larger values of strain, the <100> oriented mass reduction begins to saturate.

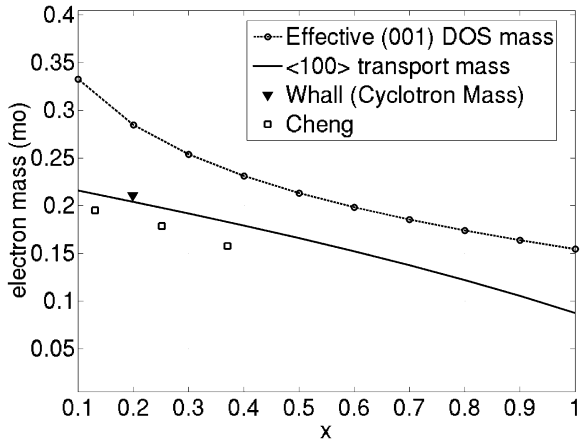

Figure 6. Calculated transport and DOS effective mass for $Si_{1-x}Ge_x$/(100)Si. Expt. Data for m_t <100> from [14] [15].

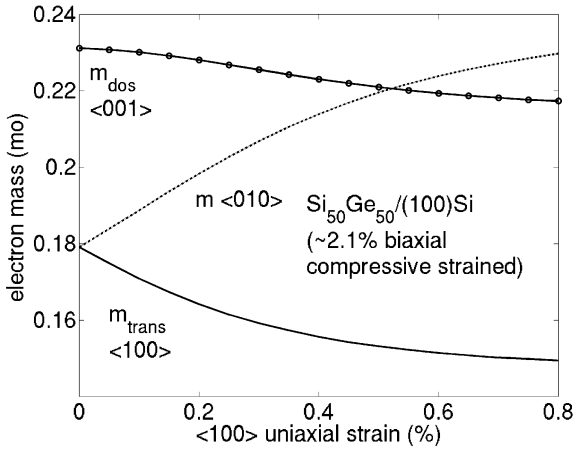

Figure 7. Calculated transport and DOS effective mass for $Si_{50}Ge_{50}$/(100)Si with uniaxial strain along <100>.

V. UNIAXIAL STRAIN IN DEVICE PERFORMANCE

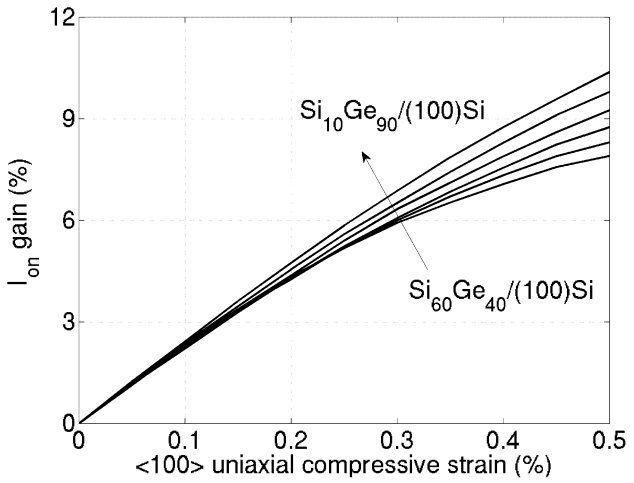

Figure 8. Current gain SiGe/Si pMOS devices due to uniaxial strain.

For more than a decade Strain has played an integral role in improving device performance. It has been shown that compressive strain improves the pMOS device performance. We analyze further possible improvements with compressive uniaxial strain to an already biaxial strained SiGe channel material. For velocity saturated MOSFETs we have[16],

$$I_{ON} \propto q.N_{2D}.v_{inj} \propto m_{dos}/\sqrt{m_{trans}} \qquad (5)$$

Using (5), the current gain is estimated in $Si_{1-x}Ge_x/Si$ type of devices for $0.4<x<0.9$. We took $x>0.4$ to be sure that the top two valence bands were sufficiently decoupled and inter-valley scattering can be safely neglected in this analysis. It is seen that for small values of uniaxial strain, the current gain is linear for all x. At higher strain values (~0.5%), the current gain depends on Ge% of the original structure. Higher Ge concentrations leads to higher performance gains at a particular strain value. About 10% device performance improvement is expected at high Ge (90%) concentration devices.

VI. CONCLUSION

A Tight-binding based bandstructure model for SiGe material was presented. The bandstructure data were benchmarked against experimental data wherever possible. We obtained a good agreement with experiments validating our model. We further analysed pMOS device performance improvements with the application of <100> uniaxial strain. Our results suggest that compressive uniaxial strain further improves biaxially strained SiGe/Si pMOS devices. About 10% current gain is estimated at high (~90) Ge concentrations.

REFERENCES

[1] L. Gomez, P. Hashemi,J. L. Hoyt, "Enhanced Hole Transport in Short-Channel Strained-SiGe p-MOSFETs," *Electron Devices, IEEE Transactions on* , vol.56, no.11, pp.2644-2651, Nov. 2009

[2] S. Takagi, T. Iisawa, T. Tezuka, Numata, T, et al "Carrier-Transport-Enhanced Channel CMOS for Improved Power Consumption and Performance," *Electron Devices, IEEE Transactions on* , vol.55, no.1, pp.21-39, Jan. 2008.

[3] A. Paul, S. Mehrotra, M. Luisier, G. Klimeck, "Performance Prediction of Ultrascaled SiGe/Si Core/Shell Electron and Hole Nanowire MOSFETs," *Electron Device Letters, IEEE* , vol.31, no.4, pp.278-280, April 2010.

[4] D. V. Lang, et. al., "Measurement of the band gap of GexSi(1-x)/Si strained-layer heterostructures," Appl. Phys. Lett. 47, 1333, 1985.

[5] D. Dutartre, "Excitonic photoluminescence from Si-capped strained Si1-xGex layers," *Phys Rev B*, vol. 44, no. 20, pp 11525, Nov. 1991.

[6] Braunstein R, Moore A R and Herman F 1958 *Phys. Rev.* 109 695–710

[7] T. B. Boykin, G. Klimeck and F. Oyafuso, "Valence Band Effective-Mass Expressions in the sp3d5s* Empirical Tight-Binding Model Applied to a Si and Ge Parametrization," *Phys. Rev. B*, vol. 69, 115201/1-10, Mar. 2004.

[8] T. B. Boykin et al, "Diagonal parameter shifts due to nearest-neighbor displacements in empirical tight-binding theory," *Phys. Rev. B, Condens. Matter*, vol. 66, no. 12, p. 125 207, Sep. 2002.

[9] Semicondctors: Group IV Elements and III-V Compunds, edited by O. Madelung (Springer,New York, 1991)

[10] J. F. Morar, P. E. Batson, and J. Tersoff, "Heterojunction band discontinuity in Si-Ge alloys using spatially resolved electron-energy-loss spectroscopy," *Phys. Rev. B*, vol. 47, pp. 4107-4110, 1993.

[11] L. Yang et. al. "Si/SiGe heterostructure parameters for device simulations," *Semicond. Sci. Technol.*, vol. 19, pp. 1174, Oct. 2004.

[12] J. Hoyt, et. al, "Evaluation of the valence band discontinuity of $Si/Si_{1-x}Ge_x/Si$ heterostructures by application of admittance spectroscopy to MOS capacitors," *Electron Devices, IEEE Transactions on*, vol.45, no.2, pp.494-501, Feb 1998.

[13] D. J. Robbins et. al., "Near-band-gap photoluminescence from pseudomorphic $Si_{1-x}Ge_x$ single layers on silicon," J. Appl. Phys. 71, 1407, 1992.

[14] T. E. Whall, A. D. Plews, N. L. Mattey,P. J. Phillips, U. Ekenberg, "Effective mass and band nonparabolicity in remote doped Si/Si0.8Ge0.2 quantum wells," *Applied Physics Letters* , vol.66, no.20, pp.2724-2726, May 1995

[15] J. P. Cheng, V. P. Kesan, D. A. Grutzmacher, and T. O. Sedgwick,," Cyclotron resonance studies of two-dimensional holes in strained Si1-xGex/Si quantum wells"Appl.Phys. Lett. 64, 1681,1994.

[16] A. Rahman, J. Guo; S. Datta, M.S. Lundstrom, "Theory of ballistic nanotransistors," *Electron Devices, IEEE Transactions on* , vol.50, no.9, pp. 1853- 1864, Sept. 2003.